FISEVIER

Contents lists available at ScienceDirect

Arthropod Structure & Development

journal homepage: www.elsevier.com/locate/asd



Micro-computed tomography of pupal metamorphosis in the solitary bee *Megachile rotundata*



Bryan R. Helm ^{a, *}, Scott Payne ^b, Joseph P. Rinehart ^c, George D. Yocum ^c, Julia H. Bowsher ^a, Kendra J. Greenlee ^a

- ^a Department of Biological Sciences, North Dakota State University, Fargo, ND 58108-6050, USA
- ^b Electron Microscopy Center, North Dakota State University, Fargo, ND 58108-6050, USA
- ^c Agricultural Research Service, Insect Genetics and Biochemistry, United States Department of Agriculture, Fargo, ND 58102-2765, USA

ARTICLE INFO

Article history: Received 22 January 2018 Accepted 9 May 2018 Available online 28 June 2018

Keywords:
Development
Metamorphosis
Micro-computed tomography
Megachile rotundata

ABSTRACT

Insect metamorphosis involves a complex change in form and function. In this study, we examined the development of the solitary bee, $Megachile\ rotundata$, using micro-computed tomography (μ CT) and volume analysis. We describe volumetric changes of brain, tracheae, flight muscles, gut, and fat bodies in prepupal, pupal, and adult M rotundata. We observed that individual organ systems have distinct patterns of developmental progression, which vary in their timing and duration. This has important implications for commercial management of this agriculturally relevant pollinator.

© 2018 The Author(s). Published by Elsevier Ltd. This is an open access article under the CC BY-NC-ND license (http://creativecommons.org/licenses/by-nc-nd/4.0/).

1. Introduction and background

An emerging model insect for understanding the effects of environmental conditions on metamorphic development is the alfalfa leafcutting bee, *Megachile rotundata* (Hymenoptera: Megachilidae). *M. rotundata* is a widely-distributed solitary bee pollinator that is commercially-reared and used to enhance production of crops, primarily alfalfa seed, *Medicago sativa* (Pitts-Singer and Cane, 2011). A common problem in managing *M. rotundata* is that populations must be synchronized with flowering of crops in different geographic locations across North America for both effective pollination and population maintenance (Bosch and Kemp, 2005; Pitts-Singer and Bosch, 2010; Pitts-Singer and Cane, 2011).

Synchronization of *M. rotundata* emergence with flowering is achieved by interrupting metamorphosis of developing bees with temperature treatments below which development stops (Pitts-Singer and Cane, 2011; Yocum et al., 2010). However, a number of studies have demonstrated that low temperature-mediated interruption of metamorphosis results in deleterious sub-lethal effects

(Bennett et al., 2015; Torson et al., 2017; Yocum et al., 2010). These effects may be shaped by the timing of the low-temperature exposure with respect to metamorphosis progression (Rinehart et al., 2016; Yocum et al., 2010). Chill injury, perturbation of developmental processes, or both are suspected mechanisms for these injuries. While the external developmental changes that occur during metamorphosis in *M. rotundata* have been characterized (Kemp and Bosch, 2000; Yocum et al., 2010), development of internal systems has not been investigated. Better spatial and temporal descriptions of internal development may help identify better timing for low-temperature exposure that minimizes negative effects for this species.

An emerging technology for characterizing both internal and external morphology of arthropods is micro-computed tomography, μ CT (Lowe et al., 2013; Metscher, 2009). μ CT generates highly resolved 3-dimensional models of internal and external anatomies when performed on insect samples. To this end, μ CT has been used successfully to compare morphology among various organisms (Metscher, 2009), including comparisons of physiological systems during insect metamorphosis (Hall et al., 2017; Lowe et al., 2013; Martin-Vega et al., 2017a, 2017b) and adult bees (Greco et al., 2008).

In this study, we used μ CT to build a more robust description of internal changes during metamorphosis in the solitary bee, *M. rotundata*. Whole organism μ CT imaging was conducted on 6

E-mail address: bryan.r.helm@ndsu.edu (B.R. Helm).

Corresponding author.

individuals, each representing a sub-stage of metamorphosis. We compare and contrast the changes in the structure of discernible, internal features across these stages. The primary aim was to determine which organ systems were developing when metamorphosis is commonly interrupted by the low-temperature methods described above.

2. Materials and methods

2.1. Study organism

Overwintering prepupal M. rotundata were obtained from JWM Leafcutters, Inc. (Nampa, ID) in the spring of 2014. Prepupae were stored in a 6 °C environmental chamber (Conviron, Winnipeg, Manitoba), which maintained a developmentally quiescent state, until the beginning of the study. Six prepupae were removed from storage and placed into a 29 °C environmental chamber (Precision Scientific, Buffalo, New York) to initiate metamorphic development. One individual was sampled for µCT scanning one day following placement into 29 °C (Fig. 1: prepupa). The prepupal stage generally lasts for 1 week before individuals pupate (Kemp and Bosch, 2000). Pupae were sampled 1, 7, 14, and 21 days following pupation (Fig. 1). These time points correspond roughly to previously used reference stages: early pupa, pink eve, red eve, and emergence ready (Yocum et al., 2010). These developmental descriptions are labeled onto the stage sampling and corresponding external development for comparative purposes in Fig. 1. One additional sample was taken of an adult male that had completed metamorphosis to the adult form but not yet emerged. Samples were removed from their brood cells immediately before scans by carefully cutting the "top" of the brood cell open with a safety razor.

2.2. Scanning procedures

Samples were dissected from leaf pods using a safety razor. The cap of the brood cell was first circumscribed with an incision. Then, the cap was removed and the individual was removed carefully with soft, curved forceps. Each sample was placed into a Kapton®

tube that was affixed to a glass rod. Samples were then scanned using a GE Phoenix v|tome|x s X-ray computed tomography system equipped with a 180 kV high power nanofocus X-ray tube with a molybdenum target and a high contrast GE DXR250RT flat panel detector (GE Sensing & Inspection Technologies GmbH, Wunstorf, Germany). Initial beam parameters were standardized for each sample; however, these beam settings were adjusted to optimize outputs for each individual sample and are provided in Supplemental Table 1. Following scans, samples were removed from the tubing and monitored for survival for 3 days. No bee completed development following the scan. This may have been from x-ray exposure, handling, or rearing conditions outside of the cocoon.

2.3. Analysis of μCT data

We focused our analysis to examine the flight musculature, the gut, the tracheae, brain, and fat bodies, because they were discernible from scans of pupae without fixation or staining (Fig. 2), although not all structures were observed in the prepupa and adult. X-ray images were aligned and optimized using automated protocols within GE Datos|x software (GE Sensing & Inspection Technologies GmbH, Wunstorf, Germany), and volumetric data were computed from stacks of x-ray images (Supplemental Fig. 1). Volumetric data were then exported to VGStudio MAX 3.0 analysis software (Volume Graphics Inc., Heidelberg, Germany) for editing and analysis. Data volumes were analyzed using 3D-segmentation and volume analysis tools in VGStudio MAX. Several segmentation tools were applied to remove unwanted components of the CT volume, such as the Kapton® tubing and mounting glass rod. Focal structures were segmented as regions of interest.

Once flight musculature, gut, tracheae, brain, and fat bodies were segmented, measurements of each structure as well as whole body volumes were calculated. Analyzed volumes were then rendered into 3D models, and images were generated of the dorsal, lateral, and ventral perspectives. Volumes of structures were then calculated as a total percentage of body volume and compared among different stages. Because only one sample was used at each stage, statistical analysis was not conducted.

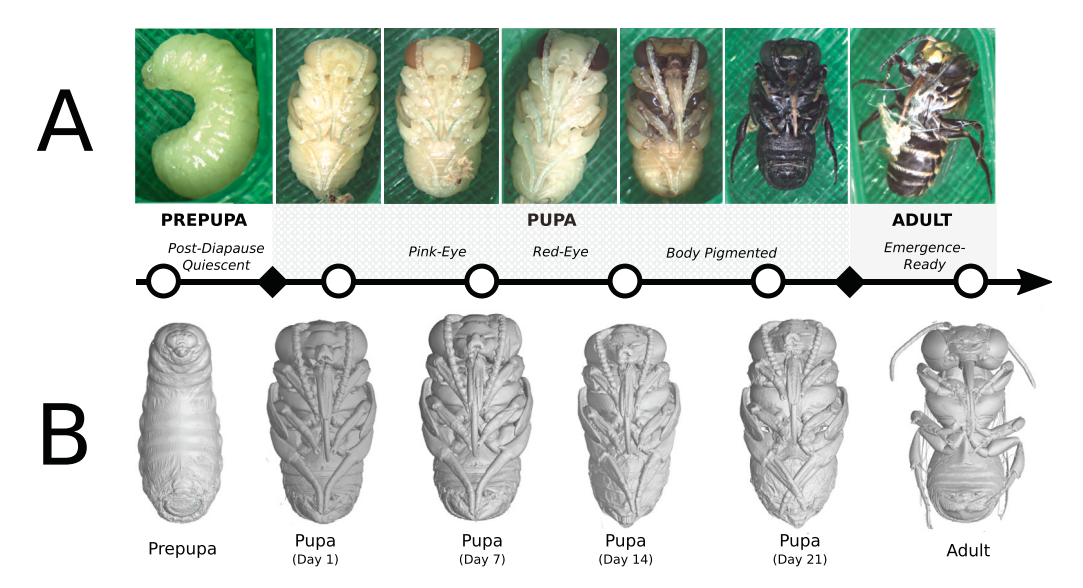


Fig. 1. External stages of metamorphosis in *M. rotundata* (A) used for sampling and their stage descriptions based on prior literature (italicized labels). Individuals were sampled during the early prepupal stage, throughout the pupal stage and in an un-emerged adult (B). The relative timing of pupal and adult eclosion are noted on the timeline (diamonds). Terms used for different stages are labeled with corresponding pupal development times (italics).

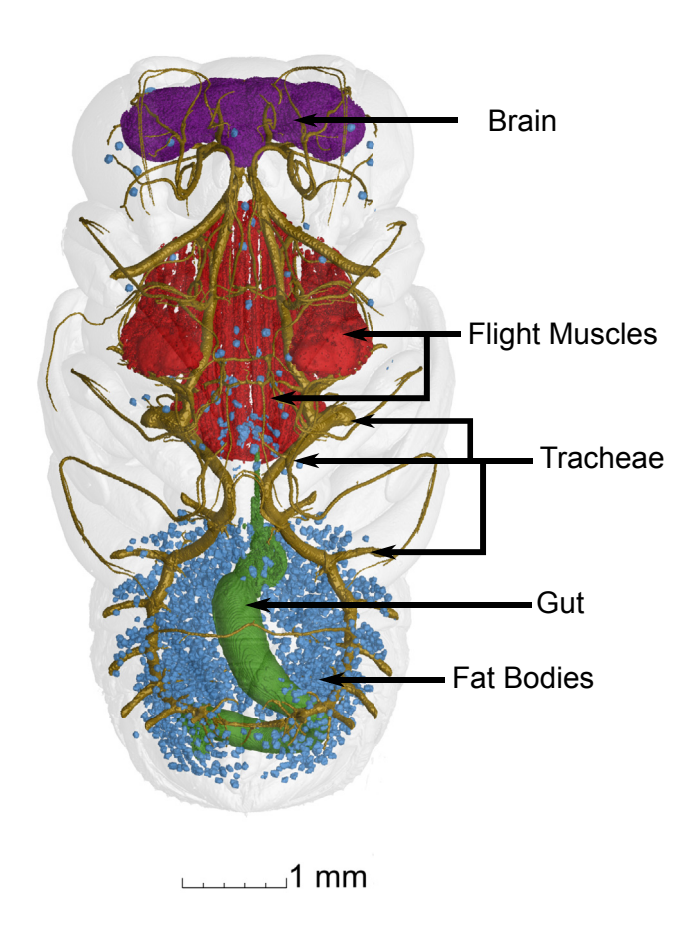


Fig. 2. Examples of brain (purple), flight muscle (red), tracheae (yellow), gut (green), and fat bodies (blue) when segmented during CT analysis.

3. Results and interpretation

3.1. Brain

Brain volumes were segmented 1 in pupal scans (Fig. 3), but brain structures were not resolved compared to methods that have used fixation and staining (Sombke et al., 2015). The brain could not be segmented in the prepupal scan. However, on day 1 of the pupal period, the general shape of the brain could be discerned and segmented from surrounding tissues (Fig. 4A) and was observed in different individuals until the end of the pupal stage (Fig. 3). Brain volumes were estimated to be $1.84 \pm 0.11\%$ of body volume and only varied in volume by $\pm 0.54\%$ of body volume throughout the pupal period (Table 1). Brain volume was not segmented in the adult scan, but the brain and eye structures were visually observable (Fig. 4B).

3.2. Tracheae

Tracheae are accurately imaged by μ CT because they are airfilled, which provides a strong contrast from surrounding tissues (Shaha et al., 2013). Tracheae were segmented in all scans from prepupa to adult (Fig. 3). Overall structure of the tracheae was simplest in the prepupal stage and grew in complexity and volume at pupation (Fig. 3). From the prepupal to the pupal stage, the

volume of tracheae increased from 0.51% to 0.88% of body volume (Fig. 3). During the pupal stage, tracheal volume decreased by nearly 50% in the day 14 pupa (Fig. 3), and many of the major tracheae in the preceding and subsequent pupal scans were not visible (Fig. 3). At this stage, lateral tracheae were no longer connected between segments, and many terminal branches were not present compared to other scans (Fig. 3).

To understand how well these measurements captured the volume of the tracheal systems, we measured the terminal ends of abdominal tracheae and found that algorithmic/manual segmentation of tracheae reliably detected air-filled tracheal branches with a diameter as small as 0.02 mm. Smaller air spaces were sometimes observable, but for those, segmentation was not possible or not reliable. This excluded some air-filled tracheae that were smaller, but not reliably segmented by contrast differences between air and tissue. Also, reliability of segmentation for small tracheae is partially shaped by how deep they were in the sample. Tracheae with closer proximity to the outer surface of the sample were more reliably segmented than those that occurred deeper in the sample.

The largest change in tracheal volume occurred between the melanized pupal stage and the adult stage. Tracheal volumes increased from 0.83% of body volume at the pupal—adult transition to 11.20% of body volume in the adult (Fig. 3, Table 1). Tracheae of the legs, thorax, and head increased in their width during this stage (Fig. 3). Tracheae of the flight muscles, which were absent in preceding stages became visible and contributed to the observed volume increase (Fig. 3).

3.3. Flight muscle

Flight musculature was segmented in all stages from prepupa to adult (Fig. 3); although the distinct muscle bundles observed in the pupal period could not be reliably segmented from the adult scan. Undifferentiated dorsolateral and dorsoventral flight muscles were present in the prepupal and early pupal stage (Figs. 3 and 5A). These muscles differentiated into distinct flight muscle bundles that filled a larger proportion of thorax volume by the day 7 scan (Fig. 5B). Flight musculature remained similar in form for subsequent pupal scans (Fig. 3). Flight muscle volumes constitute less than 1% of body volume in the early pupa, which then grew to more than 5% by the end of pupal metamorphosis (Table 1). Flight musculature of the adult was observable, but its volume could not be as accurately segmented from this scan.

3.4. Gut

The gut was discernible in prepupal and pupal samples. The prepupal gut was oriented linearly through the thorax and abdomen (Fig. 3). The gut retained this form in the early pupal stage (Fig. 3). By day 7, the gut descended into the pupal abdomen and had coiled versus its earlier, linear form (Fig. 3). Gut volume expanded by day 14 and remained similar in form for the remainder of the pupal period (Fig. 3). The gut was observed in the adult but could not be segmented from surrounding tissues confidently.

3.5. Fat bodies

The fat bodies of *M. rotundata* are dispersed throughout the body and appear as clusters of globular structures that are suspended in the hemolymph. These structures absorbed more x-ray from surrounding soft tissues and appeared as inclusions in the resulting data volumes (Fig. 2). Fat bodies were present in every scan from prepupa to adult and varied from 0.84% to 4.21% of body volume among all stages. However, there appeared to be no consistent increase or decrease with time (Table 1). Fat bodies were

¹ Please note that the terms 'segment' and 'segmentation' here are not used in their biological meaning but in a technical sense to denote partitioning pixelated or voxelated information

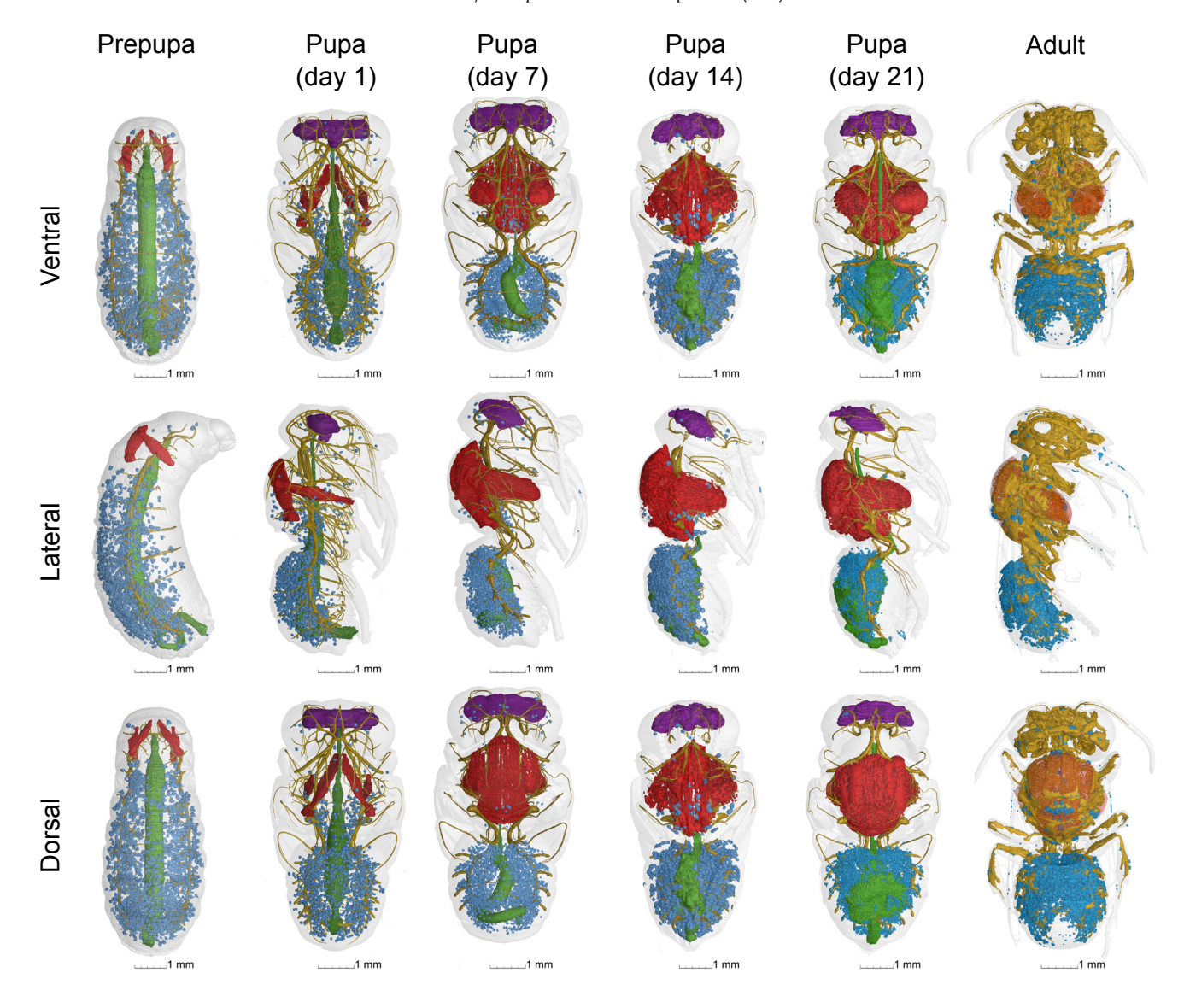


Fig. 3. Brain (purple), flight muscle (red), tracheae (yellow), gut (green), and fat bodies (blue) from different stages of metamorphosis as viewed from ventral (top row), lateral (middle row), and dorsal (bottom row) perspectives. 3-Dimensional.OBJ files are provided as supplemental files.

more abundant in the abdomen but also were observed in the thorax and head.

4. Discussion

This is the first study to characterize organogenesis of internal structures during pupal metamorphosis in the solitary bee, *M. rotundata*. At a very general level, complex patterns of organogenesis appear among different structures. In some cases, changes seem to be abrupt and associated with stage-transitions, e.g., brain appearance at pupation and tracheal growth from pupa to adult. In other cases, organ development is dissociated from clear external makers of developmental progression. This was observed for flight muscle differentiation and gut development, which showed both morphological development and volumetric growth during the early pupal stage of *M. rotundata* when external changes, such as the pigmentation of eyes, have not occurred (Fig. 1). At all stages, major changes occurred in at least one or more of the identified

organ systems, which is important knowledge when culturing these developmental stages in lab studies and commercial management.

There is a robust body of knowledge concerning the mechanisms that drive metamorphic change in holometabolous insects. Complex molecular, cellular, and endocrine mechanisms are known to regulate formation and growth of adult structures while larval tissues and energy reserves are deconstructed. Much of this knowledge is derived from relatively well-studied species where detailed knowledge about development in different organs and tissues can be compared systemically (Gilbert, 2009). μCT trades much in terms of finer mechanistic resolution for snapshots of systemic organogenesis, and recent studies have implemented this technology. Lowe et al. (2013) imaged the internal systems of the lepidopteran, *Vanessa cardui* throughout the chrysalis stage (pupal stage in the present study). Another developing insect that has been investigated using μCT during metamorphosis is the blow fly, *Calliphora vicia* (Hall et al., 2017; Martin-Vega et al., 2017a, 2017b).

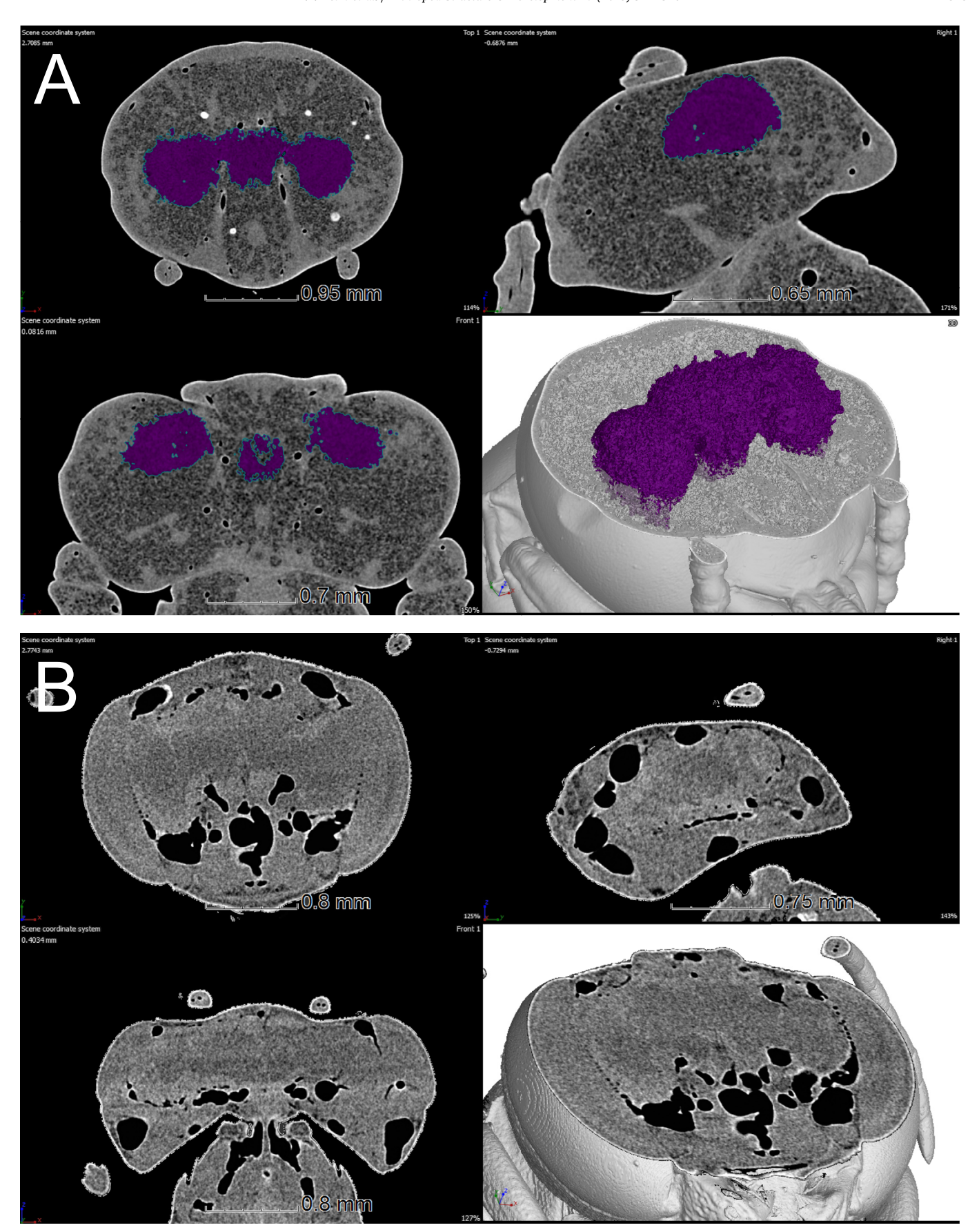


Fig. 4. Segmentation analysis of brain in pupa (A) vs adult (B). As can be seen, total brain volume can be estimated in the pupa; however the analysis could not partition brain tissue from surrounding tissues in the adult (B) even though it is slightly visible.

Table 1Summary of volumetric measures of different structures for each sample.

Stage	Body Volume mm³	Brain		Tracheae		Flight Muscles		Gut		Fat Bodies	
		mm ³	%	mm ³	%	mm ³	%	mm ³	%	mm ³	%
Prepupa	46.29	NA	NA	0.24	0.51	0.34	0.73	1.58	3.41	1.03	2.23
Pupa 1 (Day 1)	35.11	0.55	1.56	0.31	0.88	0.33	0.95	0.67	1.92	0.38	1.08
Pupa 2 (Day 7)	41.66	0.88	2.10	0.37	0.88	1.18	2.84	0.34	0.95	0.37	0.89
Pupa 3 (Day 14)	40.16	0.73	1.81	0.18	0.45	1.75	4.36	1.68	4.18	1.41	3.51
Pupa (Day 21)	44.56	0.85	1.90	0.38	0.84	2.72	6.10	1.78	3.97	0.38	0.84
Adult	23.23	NA	NA	2.60	11.21	3.14	13.52	NA	NA	0.98	4.21

Notes: Volumes and % of body mass of different structures for different stages of metamorphosis.

Interestingly, there are similarities and dissimilarities in the relative progression of organ development in these species and *M. rotundata*. For example, the formation of an air-bubble is a striking feature of metamorphosis for *V. cardui* and *C. vicia*, but no such structure appeared during *M. rotundata* metamorphosis. In *M. rotundata*, the gut was linear and uncoiled in the earliest prepupal stage and remained so through the early pupal period. The gut then regressed into the abdomen. A similar progression of gut development was observed in *V. cardui* (Lowe et al., 2013); however, the prepupal gut in *C. vicia* was already coiled in the abdomen during the feeding larval stage prior to pupation (Martin-Vega et al., 2017a, 2017b).

Because of their material composition, some structures appear clearly in some studies, but are not necessarily as apparent in others. For example, the tracheal structure of $V.\ cardui$ was segmented throughout pupal development (Lowe et al., 2013) as was the case for $M.\ rotundata$; although these data are not presented for $C.\ vicia$ (Martin-Vega et al., 2017a, 2017b). Flight musculature is described well for $C.\ vicia$ (Martin-Vega et al., 2017a, 2017b) and $M.\ rotundata$ but was not present in the scans of $V.\ cardui$ (Lowe et al., 2013). Many factors contribute to how well different tissues are imaged using μCT , resulting in discrepancies among studies. For example, the fat bodies in $M.\ rotundata$ are highly x-ray absorbent compared to surrounding materials, but such inclusions did not appear in $V.\ cardui$ or $C.\ vicia$ (Lowe et al., 2013; Martin-Vega et al., 2017a, 2017b).

Various fixation, staining, and scanning techniques have been used to enhance tissue discernibility. These techniques may also limit how well target features appear in scans. For M. rotundata, flight muscles were undifferentiated during the prepupal and pupal stages but subsequently differentiated into large bundles of flight muscles by the mid-pupal period (Figs. 3 and 4). Brain tissues were not discernible in the prepupal sample; however, the general brain outline could be segmented in the pupal stage. The resolution of neural tissues can be enhanced greatly by the use of fixation and staining (Sombke et al., 2015). However, we chose not to use staining in this study here, because some of the focal structures do not appear after fixation and staining (i.e., tracheae). Although the brain was observed in adult scans (Fig. 4), the lack of contrast with surrounding tissues and newly apparent tracheal air sacs make its segmentation intractable compared to pupal stages. As noted above, fat bodies appeared as globular structures that absorbed far more x-ray than surrounding tissues, suggesting that something about their composition increased xray absorption. We suspect that fat bodies may contain urocytes, fat body cells that store nitrogenous wastes (Arrese and Soulages, 2010).

There are several limitations for the present study. For one, there is a small sample size and no resampling for each day. While scanning procedures are generally straightforward with current systems, the segmentation and analysis of data volumes is

not always straight forward. Also, the data are presented without fixation or staining procedures. Although these techniques enhance resolution of internal structures and accuracy of measurements (Metscher, 2009), they also result in shrinking of structures and obscure the tracheae in insect samples (Helm, personal observation). Therefore, we opted to trade enhanced resolution for the ability to visualize the tracheal system in vivo. It would be interesting to compare individuals stained with those that were unstained. In addition, more robust x-ray and detector capabilities, such as those used for phase-contrast XCT, could provide quicker scanning times and enhanced contrast images, which may produce better tomographic data sets more rapidly (Walton et al., 2015; Xu et al., 2016). Compared to older techniques, such as tissue fixation and cryo-slicing, μCT produces in vivo positioning of major organs, but does not have the fine resolution of ultrastructures. Also, our primary metric of developmental change was volumetric measurements. While these measurements offer a consistent variable to measure among samples, morphometric changes are occurring simultaneously. Classic, multivariate morphometric approaches could be useful for assessing developmental changes with sufficient sample sizes. One final consideration is that females and males progress through development at different rates but this difference was not accounted for because sex was not known in the scan preparations. Future work could possibly identify characteristics that are sexually dimorphic and characterize organogenesis separately.

Knowing the complex nature of developmental progression for different organ systems in M. rotundata poses significant new challenges in terms of their management. For one, interrupting metamorphic development as is done for emergence synchronization with flowering plants could have unique effects at each stage because the organ systems are at different stages of organogenesis throughout metamorphosis. For example, an early pupa placed into cold storage may be more vulnerable to damage of the flight muscle or gut, because those systems are in the early stages of development. Placing a later pupal stage into cold storage would possibly affect entirely different organ systems in different mechanistic ways. At that time, some systems are already fully formed, which could make them susceptible to irreparable chill injuries. Differences in the relative developmental progress of these specific anatomical systems may explain stage-specific susceptibilities to low temperature exposure and could account for previously observed sub-lethal effects. Bennett et al. (2015) identified distinct alterations of flight performance when M. rotundata were interrupted 14 days following removal from overwintering conditions. This corresponds to the stage when flight muscles differentiate (Fig. 3). Perhaps prolonged cold exposure during this phase of metamorphosis disrupts flight muscle formation to cause reduced flying metabolic rates and/or complete disruption of flight ability (Bennett et al., 2015).

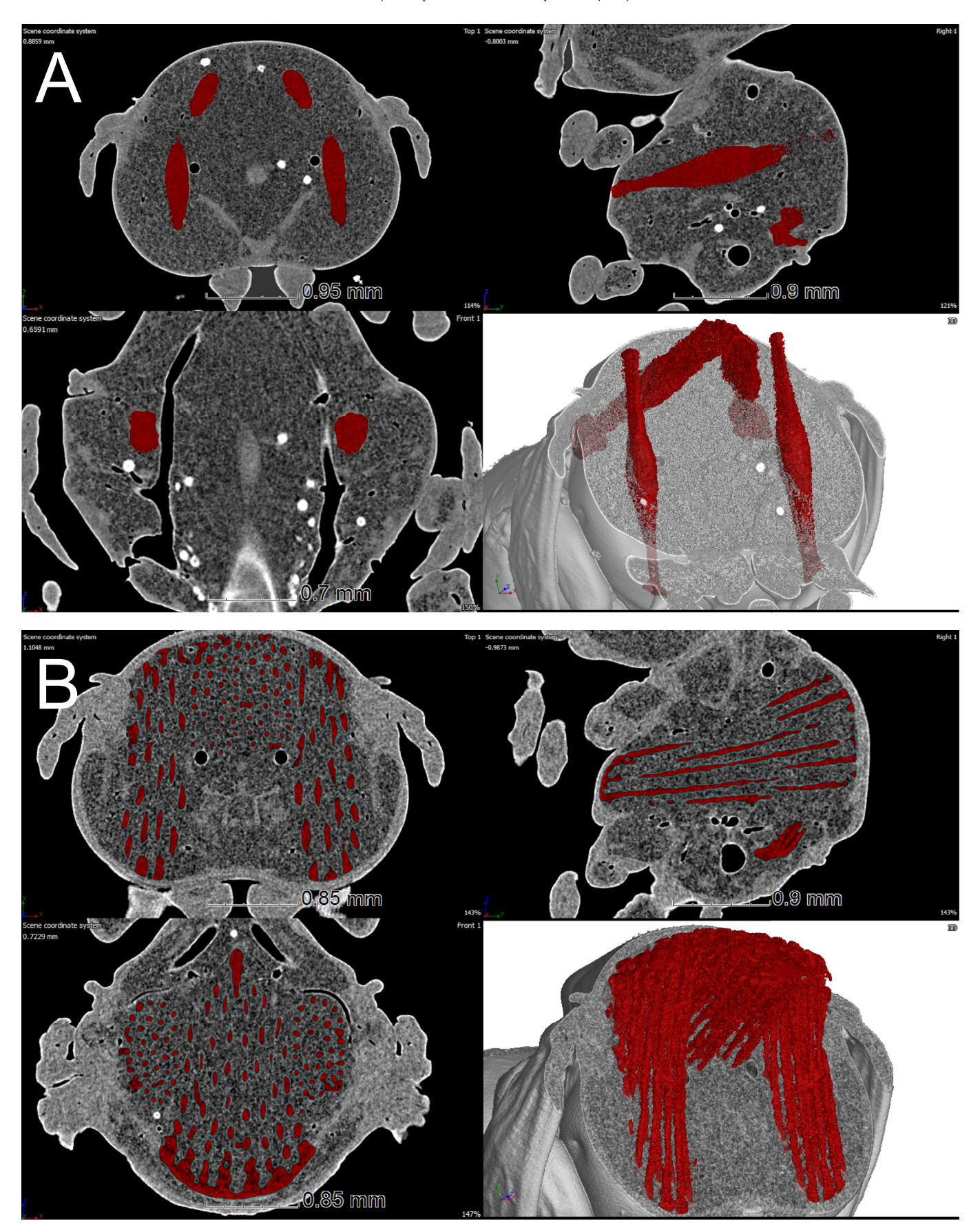


Fig. 5. Segmentation analysis of flight muscle when undifferentiated in early pupal (A) vs differentiated in mid-pupal period (B).

5. Conclusion

Describing the metamorphosis of *M. rotundata* is important because of its role as a commercially-managed pollinator. Understanding the important changes that are occurring during metamorphosis permits more informed scientific study and commercial practices when rearing bees. Micro-computed tomography can produce incredible information about the changes that occur during metamorphosis, as we have described here for *M. rotundata*.

Acknowledgements

We would like to thank M. Faillace and J. Moore for their training and assistance conducting this work. This study was supported by the USDA-ARS in Insect Genetics and Biochemistry, NSF MRI-122417 to KJG, NSF IOS-0953297 to KJG, and North Dakota State University Department of Biological Sciences in Fargo, ND.

Appendix A. Supplementary data

3-dimensional .OBJ files of CT are available as supplemental files to the manuscript.

Supplementary data related to this article can be found at https://doi.org/10.1016/j.asd.2018.05.001.

Author contributions

BRH designed and conducted study, analyzed data, and wrote the manuscript. SP conducted the study, helped analyze data, and contributed to manuscript writing. KJG and JHB assisted with experimental design, provided funding, and edited the manuscript. GDY and JPR provided bees, advised the study, and contributed to manuscript writing.

References

- Arrese, E.L., Soulages, J.L., 2010. Insect fat body: energy, metabolism, and regulation. Annu. Rev. Entomol. 55, 207–225. https://doi.org/10.1146/annurev-ento-112408-085356.
- Bennett, M.M., Cook, K.M., Rinehart, J.P., Yocum, G.D., Kemp, W.P., Greenlee, K.J., 2015. Exposure to suboptimal temperatures during metamorphosis reveals a critical developmental window in the solitary bee, *Megachile rotundata*. Physiol. Biochem. Zool. 88, 508–520. https://doi.org/10.1086/682024.
- Bosch, J., Kemp, W.P., 2005. Alfalfa leafcutting bee population dynamics, flower availability, and pollination rates in two Oregon alfalfa fields. J. Econ. Entomol. 98, 1077–1086.
- Gilbert, L.J., 2009. Insect Development: Morphogenesis, Molting, and Metamorphosis, first ed. Elsevier, Burlington, MA.

- Greco, M., Jones, A., Spooner-Hart, R., Holford, P., 2008. X-ray computerised microtomography (MicroCT): a new technique for assessing external and internal morphology of bees. J. Apic. Res. Bee World 47, 286–291. https://doi.org/ 10.3896/IBRA.1.47.4.09.
- Hall, M.J.R., Simonsen, T.J., Martín-vega, D., 2017. The "dance" of life: visualizing metamorphosis during pupation in the blow fly *Calliphora vicina* by X-ray video imaging and tomography subject category: subject areas.
- Kemp, W.P., Bosch, J., 2000. Development and emergence of alfalfa pollinator Megachile rotundata. Ann. Entomol. Soc. Am. 93, 904–911.
- Lowe, T., Garwood, R.J., Simonsen, T.J., Bradley, R.S., Withers, P.J., 2013. Metamorphosis revealed: time-lapse three-dimensional imaging inside a living chrysalis. J. R. Soc. Interface 10, 20130304. https://doi.org/10.1098/rsif.2013.0304
- Martin-Vega, D., Simonsen, T.J., Hall, M.J.R., 2017a. Looking into the puparium: micro-CT visualization of the internal morphological changes during metamorphosis of the blow fly, *Calliphora vicina*, with the first quantitative analysis of organ development in cyclorrhaphous dipterans. J. Morphol. 278, 629–651. https://doi.org/10.1002/jmor.20660.
- Martin-Vega, D., Simonsen, T.J., Wicklein, M., Hall, M.J.R., 2017b. Age estimation during the blow fly intra-puparial period: a qualitative and quantitative approach using micro-computed tomography. Int. J. Leg. Med. 1429–1448. https://doi.org/10.1007/s00414-017-1598-2.
- Metscher, B.D., 2009. MicroCT for comparative morphology: simple staining methods allow high-contrast 3D imaging of diverse non-mineralized animal tissues. BMC Physiol. 9, 11. https://doi.org/10.1186/1472-6793-9-11.
- tissues. BMC Physiol. 9, 11. https://doi.org/10.1186/1472-6793-9-11. Pitts-Singer, T.L., Bosch, J., 2010. Nest establishment, pollination efficiency, and reproductive success of *Megachile rotundata* (Hymenoptera: Megachilidae) in relation to resource availability in field enclosures. Environ. Entomol. 39, 149–158. https://doi.org/10.1603/EN09077.
- Pitts-Singer, T.L., Cane, J.H., 2011. The alfalfa leafcutting bee, *Megachile rotundata*: the world's most intensively managed solitary bee. Annu. Rev. Entomol. 56, 221–237. https://doi.org/10.1146/annurev-ento-120709-144836.
- Rinehart, J.P., Yocum, G.D., Kemp, W.P., Bowsher, J.H., 2016. Optimizing fluctuating thermal regime storage of developing Megachile rotundata (Hymenoptera: Megachilidae). J. Econ. Entomol. 109, 993–1000. https://doi.org/10.1093/jee/ tow026
- Shaha, R.K., Vogt, J.R., Han, C.-S.S., Dillon, M.E., 2013. A micro-CT approach for determination of insect respiratory volume. Arthropod Struct. Dev. 42, 437–442. https://doi.org/10.1016/j.asd.2013.06.003.
- Sombke, A., Lipke, E., Michalik, P., Uhl, G., Harzsch, S., 2015. Potential and limitations of X-Ray micro-computed tomography in arthropod neuroanatomy: a methodological and comparative survey. J. Comp. Neurol. 523, 1281–1295. https:// doi.org/10.1002/cne.23741.
- Torson, A.S., Yocum, G.D., Rinehart, J.P., Nash, S.A., Kvidera, K.M., Bowsher, J.H., 2017. Physiological responses to fluctuating temperatures are characterized by distinct transcriptional profiles in a solitary bee. J. Exp. Biol. https://doi.org/ 10.1242/jeb.156695 jeb.156695.
- Walton, L.A., Bradley, R.S., Withers, P.J., Newton, V.L., Watson, R.E.B., Austin, C., Sherratt, M.J., 2015. Morphological characterisation of unstained and intact tissue micro-architecture by X-ray computed micro- and nano-tomography. Sci. Rep. 5, 1–14. https://doi.org/10.1038/srep10074.
- Xu, L., Chen, R., Du, G., Yang, Y., Wang, F., Deng, B., Xie, H., Xiao, T., 2016. Anisotropic shrinkage of insect air sacs revealed in vivo by X-ray microtomography. Sci. Rep. 6, 1–7. https://doi.org/10.1038/srep32380.
- Yocum, G.D., Rinehart, J.P., West, M., Kemp, W.P., 2010. Interrupted incubation and short-term storage of the alfalfa pollinator *Megachile rotundata* (Hymenoptera: Megachilidae): a potential tool for synchronizing bees with bloom. J. Econ. Entomol. 103, 234–241. https://doi.org/10.1603/EC09351.